Published in final edited form as:

Cell Rep. 2015 August 11; 12(6): 1019–1031. doi:10.1016/j.celrep.2015.07.003.

Serine 62 phosphorylated MYC associates with nuclear lamins and its regulation by CIP2A is essential for regenerative proliferation

Kevin Myant[1,*,§], **Xi Qiao**[2,3,*], **Tuuli Halonen**[2], **Christophe Come**[2], **Anni Laine**[2], **Mahnaz Janghorban**[4], **Johanna I. Partanen**[5], **John Cassidy**[1], **Erin-Lee Ogg**[1], **Patrizia Cammareri**[1], **Tiina Laiterä**[2], **Juha Okkeri**[2], **Juha Klefström**[5], **Rosalie C. Sears**[4], **Owen J. Sansom**[1,#], and **Jukka Westermarck**[2,3,#]

[1]The Beatson Institute for Cancer Research, Glasgow, G61 1BD, UK [2]Turku Centre for Biotechnology, University of Turku and Åbo Akademi University, 20520 Turku, Finland [3]Department of Pathology, University of Turku, 20520 Turku, Finland [4]Department of Molecular and Medical Genetics and Knight Cancer Institute, Oregon Health & Science University, Portland, Oregon 97239, USA [5]Research Programs Unit, Translational Cancer Biology & Institute of Biomedicine, 00014 University of Helsinki, Finland

SUMMARY

Understanding of the mechanisms determining MYC's transcriptional -and proliferation promoting activities *in vivo* could facilitate approaches for MYC targeting. However, post-translational mechanisms that control MYC function *in vivo* are poorly understood. Here we demonstrate that MYC phosphorylation at serine 62 enhances MYC accumulation on Lamin A/C-associated nuclear structures and the Protein Phosphatase 2A (PP2A) inhibitor protein CIP2A is required for this process. CIP2A is also critical for serum induced MYC phosphorylation, and for MYC-elicited proliferation induction *in vitro*. Complementary transgenic approaches and an intestinal regeneration model further demonstrated the *in vivo* importance of CIP2A and serine 62

Correspondence should be addressed to O.J.S or J.W: (o.sansom@beatson.gla.ac.uk or jukwes@utu.fi).
*These authors contributed equally to this work
#These senior authors contributed equally to this work
§Current address: Edinburgh Cancer Research Centre, IGMM, Edinburgh, EH4 2XU, UK.

SUPPLEMENTAL INFORMATION

Supplemental information includes 6 figures and supplemental experimental procedures.

AUTHOR CONTRIBUTIONS

K.M contributed to Fig. 4A,D,E; Fig. 5, Fig. 6, Fig. 7. Fig. S4. X.Q. contributed Fig. 1A,C,D,E,F,G,I,J; Fig. 2C,F,G; Fig. 4B,C,D,E,F; Fig. 7F; Fig. S1A; Fig. S2. T.H. contributed to Fig. 1B,H; Fig. 2A,D; Fig. 3E; Fig. S1B; Fig. S5. C.C. contributed to development and characterization of CIP2A^{HOZ} mouse strain. A.L. contributed to Fig. 3A,B,C,D,F,G,I; Fig. S3. M.J. contributed to Fig. 6E,F; Fig. 7B,C. J.I.P contributed to Fig. 3H,I. J.C, E-L.O and P.C all contributed to tissue analysis of transgenic mouse models. T.L. contributed to Fig. 3A,F,G. J.O. contributed to supervision and data analysis. J.K contributed to experimental planning, data analysis and manuscript writing. R.C.S provided the MYC phosphorylation mutant mice and contributed to experimental planning, data analysis. O.J.S. contributed to supervision, concept and experiment planning, data analysis and manuscript writing. J.W. contributed to supervision, concept and experiment planning, data analysis and manuscript writing.

phosphorylation for MYC activity upon DNA damage. However, targeting of CIP2A did not influence normal function of intestinal crypt cells. The data underline the importance of nuclear organization in the regulation of MYC phosphorylation, leading to *in vivo* demonstration of a strategy for inhibiting MYC activity without detrimental physiological effects.

Graphical Abstract

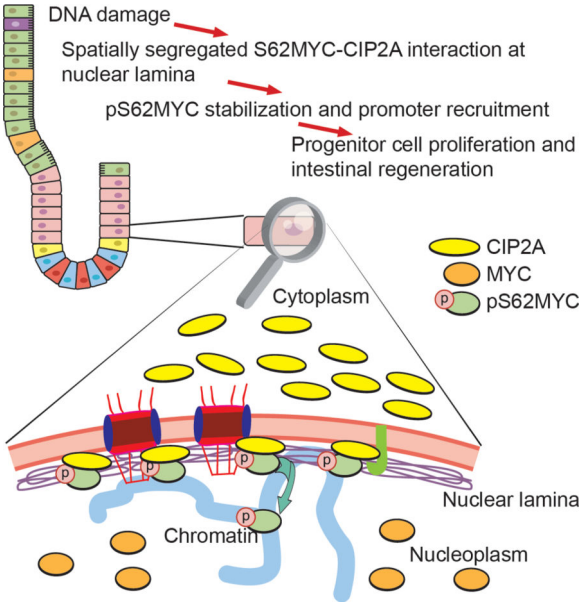

INTRODUCTION

Understanding of the mechanisms controlling MYC function *in vivo* is critical for development of MYC-targeted therapies. By using loss-of-function genetic models, MYC has been shown to be required for proliferation induction in several types of normal cells, including fibroblasts, intestinal progenitors and lymphoid B- and T-cells (de Alboran et al., 2001; Mateyak et al., 1997; Sansom et al., 2007; Trumpp et al., 2001). Moreover, it has been recently demonstrated that MYC expression is essential for intestinal crypt regeneration in response to either irradiation –or chemically induced DNA damage (Ashton et al., 2010; Athineos and Sansom, 2010). Although these studies have convincingly demonstrated the critical role for MYC dose for *in vivo* proliferation response, they are not particularly informative for the understanding endogenous mechanisms that regulate MYC's activity by post-translation modifications *in vivo*.

The induction of c-*myc* mRNA expression after proliferative stimuli is very rapid and transient, whereas the expression of the MYC protein is more sustained due to increased protein stability (Hann, 2006; Lutterbach and Hann, 1994; Sears et al., 1999; Thomas and Tansey, 2011). Cell culture and *in vitro* studies have revealed that MYC protein is heavily regulated by various post-translational modifications (Hann, 2006; Luscher and Vervoorts, 2012). Moreover, several different domains of MYC are implicated to be critical for its activity in regulating expression of its numerous target genes, as well as for proliferation

regulation (Hann, 2006; Luscher and Vervoorts, 2012; Meyer and Penn, 2008). Remarkably, despite of this knowledge, it has not been established which one(s) of the numerous MYC post-translational modifications define MYC's activity *in vivo*.

Cancerous inhibitor of PP2A, CIP2A, is a recently identified human oncoprotein (Junttila et al., 2007; Khanna et al., 2013). Consistent with its role as an inhibitor of ubiquitous serine/threonine phosphatase PP2A that regulates activity of numerous cellular signalling pathways (Janssens and Goris, 2001), CIP2A has been shown to regulate phosphorylation and activity of Akt, DapK, E2F1, MYC and mTORC (Khanna et al., 2013; Puustinen et al., 2014). However, except for its role in promoting spermatogenesis (Ventela et al., 2012), the physiological role of CIP2A is unclear. Also, *in vivo*, the only thus far validated CIP2A target protein is E2F1, in murine model of breast cancer (Laine et al., 2013).

Very recent studies have demonstrated a critical function for nuclear lamina associated structures in gene regulation and chromosomal organization (Arib and Akhtar, 2011; Bukata et al., 2013; Dechat et al., 2010; Kind et al., 2013; Zullo et al., 2012). In this work, we demonstrate that serine 62 phosphorylation promotes MYC recruitment to nuclear Lamin A/C-associated structures (LAS) where its interaction with CIP2A is required for retaining this localization and MYC activity. Moreover, by using MYC loss of function and phosphorylation mutants, and the attenuation of CIP2A, we provide a comprehensive *in vivo* approach to validate the importance MYC serine 62 phosphorylation for organismal proliferation response. Together the results demonstrate endogenous mechanism that defines activating phosphorylation of MYC *in vivo*. As CIP2A is dispensable for normal tissue function and mouse well-being, these results also indicate potential therapeutic opportunities for inhibition of MYC activity *in vivo* without detrimental effects on normal physiology.

RESULTS

Characterization of spatial nuclear organization of CIP2A-MYC interaction

To provide spatial understanding to CIP2A-mediated regulation of MYC, we first analysed the subcellular distribution of CIP2A in HeLa cells in which CIP2A constitutively promotes expression of serine 62 phosphorylated MYC, and MYC activity (Junttila et al., 2007; Niemelä et al., 2012). Consistent with immunofluorescence staining analyses (Figure 1A), the great majority of CIP2A was expressed in cytoplasmic fraction (C) of cells (Figure 1B), but small fraction was expressed also in the nucleus and especially in the insoluble nuclear fraction (I) together with Lamin A/C (Figure 1B). Importantly, proximity ligation assay (PLA) with CIP2A and Lamin A/C primary antibodies revealed a clear CIP2A-Lamin A/C association (Figure 1C). Interestingly, CIP2A interaction with Lamin A/C is not restricted to nuclear lamina but is also observed in discrete intranuclear dots. This is fully consistent with immunofluorescence (IF) analysis of intranuclear localization of Lamin A/C (Figure 1C), and recently published data that many Lamin A/C containing structures are mobile in the nuclei (Capelson et al., 2010; Kind et al., 2013).

Next we used PLA to analyse whether MYC interacts with Lamin A/C. MYC-Lamin A/C association was observed with a pattern that resembled CIP2A-Lamin A/C association; the majority of signals being detected in the nuclear periphery but also very clear intranuclear

interactions were observed (Figure 1D and S1A). Importantly, the CIP2A-MYC association by PLA also co-localised with Lamin A/C at the nuclear lamina, although again also intranuclear interactions were also observed (Figure 1E, panel b and inserts). Serine 62 phosphorylation of MYC is important for MYC-mediated gene regulation and protein stability (Hann, 2006; Luscher and Vervoorts, 2012). Notably, PLA with pS62MYC antibody and CIP2A revealed a similar pattern of interaction at nuclear lamina than with antibody that detects the total MYC pool (Figure1E, panels c and d, Figure 1F), indicating that the form of MYC that interacts with CIP2A is phosphorylated on serine 62. To control that the pattern of CIP2A-pS62MYC PLA signals, both at nuclear lamina and in the nuclear interior, corresponds to distribution of pS62MYC protein, the cells were examined by pS62MYC immunofluoresence staining. As shown in figure 1G, the distribution of pS62MYC did resemble the nuclear lamina enriched punctuate pattern seen with CIP2A-pS62MYC PLA, although based on fewer CIP2A-pS62MYC PLA signals (Figure 1E), as compared to signals observed with immunofluorescence staining (Figure 1G), it is apparent that only certain fraction of pS62MYC interacts with CIP2A at any given moment. Importantly, the distribution pattern of total MYC did not show similar punctuate pattern as was observed with pS62MYC IF or by CIP2A-MYC PLA, and there was no particular enrichment of total MYC IF signals at nuclear periphery (Figure 1G). This further indicates that the form of MYC that CIP2A interacts at LAS is pS62MYC.

These results reveal a selective spatial distribution of pS62MYC in complex with CIP2A at LAS.

The major fraction of pS62MYC is bound to proteinaceous nuclear structures via a DNA-independent mechanism

Next we addressed by classical salt fractionation protocol biochemical basis of CIP2A and pS62MYC association with LAS. Expectedly, we found that increasing NaCl concentration released both pS62MYC and MYC from the insoluble to soluble nuclear fraction (Figure S1B and 1H). However, as compared with MYC, a significant fraction of CIP2A remained insoluble even in the presence of 500 mM NaCl, and as expected, H3 was entirely resistant to this treatment (Figure S1B and 1H). To further study potential role of DNA-binding in nuclear segregation of CIP2A and pS62MYC to LAS, the insoluble nuclear fractions isolated without detergent treatment were subjected to DNAase (Benzonase) treatment and expression of pS62MYC, total MYC, MAX, and CIP2A was compared between the insoluble pellet and the benzonase eluate. To control the efficacy of elution of DNA-bound proteins by benzonase, we show that approximately 70% of the total H3 was eluted by this treatment (Figures 1I and J). Surprisingly, only approximately 20% of pS62MYC, total MYC, or MAX was eluted by benzonase treatment (Figures 1I and J) whereas, in comparison to H3 and MYC, negligible amounts of CIP2A were detected from benzonase-treated eluates (Figures 1I and J).

These results indicate that CIP2A, and the majority of pS62MYC is bound to proteinaceous component of LAS. Moreover, association of pS62MYC with LAS seems to be mediated by an ionic interaction.

Serine 62 phosphorylation of MYC drives its association with LAS and CIP2A is required for retaining this localization

Based on results above we rationalized that serine 62 phosphorylation of MYC may promote recruitment of MYC to LAS, and that rather than chromatin binding, its interaction with CIP2A may be required to retain pS62MYC in these sites of chromatin re-organization and transcription regulation (Arib and Akhtar, 2011; Kind et al., 2013; Zullo et al., 2012). To study this, we examined distribution of exogenously expressed wild-type MYC and two mutants, S62A and T58A MYC, between the insoluble and soluble nuclear fractions. We have previously shown that the functionally inactive MYC S62A mutant (Benassi et al., 2006; Sears et al., 2000) does not interact with CIP2A in human cells (Junttila et al., 2007), whereas the MYC T58A mutant, which is a functional mimic of serine 62 phosphorylated MYC (Benassi et al., 2006; Hann, 2006; Wang et al., 2011; Yeh et al., 2004), retains full CIP2A interacting capacity (Junttila et al., 2007). Notably, S62A mutant of MYC showed clearly reduced accumulation to insoluble nuclear fraction as compared to wild-type MYC, whereas CIP2A binding-competent T58AMYC accumulated very efficiently in the insoluble fraction (Figures 2A and B). These results are in agreement with PLA results demonstrating that the form of MYC that is associated with LAS is pS62MYC (Figure 1E–G). To further confirm that distribution to insoluble fraction reflects differential association of MYC phosphorylation mutants with LAS, we performed a PLA assay with V5 and Lamin A/C antibodies in cells expressing equivalent amounts of V5-S62AMYC or V5-T58AMYC (Figure S2). Consistent with other results, T58AMYC showed clearly increased association with Lamin A/C as compared to S62AMYC (Figure 2C).

The results above, together with PLA and IF analysis of pS62MYC (Figure 1E and G), clearly demonstrate that serine 62 phosphorylation increases MYC's association with LAS. However, whether CIP2A is relevant for accumulation of MYC to LAS has not been addressed yet. To this end, we studied the sub-nuclear distribution of pS62MYC and total MYC in CIP2A siRNA-transfected cells. For the first part of this experiment, the nuclear proteins were extracted with low salt buffer (150 mM NaCl) to preserve MYC's association with the Lamin A/C. In support of our hypothesis, depletion of CIP2A inhibited the expression of pS62MYC in the Lamin A/C-enriched insoluble fraction, whereas expression of total MYC was inhibited to a much smaller extent (Figure 2D (compare lanes 2 and 4) and 2E, insoluble). Importantly, the soluble fraction of pS62MYC was insensitive to CIP2A inhibition (Figures 2D (lanes 1 and 3) and 2E, soluble). To confirm that the CIP2A sensitive pS62MYC pool corresponds to the salt sensitive pool of MYC described in figure 1H, insoluble proteins were extracted from CIP2A siRNA transfected cells in the presence of 400 mM salt. Also in this case, the CIP2A sensitive pool of MYC was the pS62MYC eluted from insoluble fraction (Figures 2D (lanes 5 and 7) and E).

CIP2A has been shown to prevent degradation of MYC and this effect is seen more profoundly with pS62MYC than total MYC antibody (Junttila et al., 2007). Thus, we examined whether CIP2A influences pS62MYC stability in insoluble nuclear fraction. Indeed, cycloheximide chase experiment revealed a clear decrease in the protein stability upon CIP2A RNAi in insoluble nuclear fraction, by using both pS62MYC and MYC antibody (Figure 2F). To confirm these results, we studied impact of CIP2A depletion in

insoluble nuclear fraction on T58A mutant that is resistant to PP2A-mediated destabilization (Yeh et al., 2004). Indeed, whereas CIP2A siRNA effects where observed by pS62MYC antibody that detects both endogenous MYC and T58A, CIP2A depletion did not alter accumulation of MYCT58A to insoluble nuclear fraction (Figure 2G).

Together, results thus far demonstrate a function for serine 62 phosphorylation of MYC in promoting its association with LAS. These results also demonstrate that CIP2A is not a universal regulator of MYC, but selectively supports stability of LAS-associated pool of pS62MYC. As explained later, this newly characterized selectivity of CIP2A towards spatially segregated pS62MYC may explain the lack of detrimental physiological effects of systemic CIP2A inhibition (Laine et al., 2013; Ventela et al., 2012), as compared to direct inhibition of MYC (Dubois et al., 2008; Soucek et al., 2008).

CIP2A is critical for serum-induced pS62MYC expression and for MYC-mediated proliferation induction

Next we studied the relevance of CIP2A for mitogen-induced MYC regulation in mouse embryo fibroblasts (MEFs) isolated from CIP2A deficient ($CIP2A^{HOZ}$) mice (Laine et al., 2013; Ventela et al., 2012) and their wild-type counterparts. Importantly, the loss of CIP2A clearly inhibited serum-induced expression of the serine 62 phosphorylated MYC (Figures 3A and B). As immunoblotting of the same membrane with an antibody against total MYC showed an equal impairment in MYC accumulation (Figures 3A and B), we postulate that pS62MYC is the form of MYC that is most sensitive to mitogenic stimuli. This conclusion is supported by the preferential induction of pS62MYC protein expression, as compared to total MYC, in wild type MEFs treated with increasing concentrations of serum (Figure 3C and D). Importantly, c-myc mRNA induction was not impaired in serum-induced $CIP2A^{HOZ}$ MEFs (Figure 3E), further indicating that the effects on MYC are due to a CIP2A-dependent post-translational mechanism. Moreover, $CIP2A^{HOZ}$ MEFs showed a statistically significant decrease in BrdU incorporation (Figure 3F) and in the re-initiation of the cell cycle in response to serum induction (Figure 3G), consistently with reported results (Kim et al., 2013). Notably, the effects of CIP2A loss on MEF cell cycle regulation and proliferation are not as robust as reported for MYC null MEFs (de Alboran et al., 2001; Meyer and Penn, 2008; Perna et al., 2012), which is consistent with our conclusion that CIP2A loss affects only a sub-population of MYC. To provide additional and more direct evidence that CIP2A supports MYC's ability to drive cell cycle activity, we employed conditional MYC-ER-expressing MCF-10A cells. In these cells, the addition of 4-hydroxytamoxifen activates MYC-ER, and this activation is sufficient to induce cell cycle re-entry in growth factor-deprived cultures (Nieminen et al., 2007). Notably, the inhibition of CIP2A expression resulted in the loss of the ability of tamoxifen-activated MYC-ER to promote the cell cycle (Figure 3H). Importantly, the CIP2A depletion did not affect MYC-ER fusion protein expression, confirming that CIP2A promotes MYC activity in proliferation induction (Figure 3I). Unlike in cancer cells (Laine et al., 2013), CIP2A inhibition in either MCF-10A or MEF cells did not affect E2F1 expression (Figure S3), providing further support to selective role for CIP2A in regulating MYC activity in these cells.

Together these results identify CIP2A as a critical endogenous regulator of MYC serine 62 phosphorylation and function during proliferation induction.

MYC interacts with CIP2A in mouse intestinal tissue

Intestinal regeneration after DNA-damage induced by irradiation or by cisplatin treatment is fully dependent on MYC dose and thus it can be used as a model to address MYC-dependency of *in vivo* proliferation response (Ashton et al., 2010; Athineos and Sansom, 2010; Finch et al., 2009; Muncan et al., 2006; Sansom et al., 2007). Similarly to MYC, we observed CIP2A immunopositivity in cells of the intestinal crypt, with reduced expression in the differentiated cells of the villi (Figure 4A). The specificity of this staining pattern was demonstrated by a lack of specific staining in CIP2A^{HOZ} tissue (Figure 5A). Moreover, *in situ* PLA activity as an indication of an association between CIP2A and MYC proteins was detected in the nuclei of intestinal crypt cells (Figure 4B; insert a, and Figure 4C,D). In contrast, PLA using only secondary antibodies did not produce any detectable PLA activity (Figure 4B; insert b, and Figure 4C). As an additional control, we show that in comparison to wild-type tissue, a clearly smaller number of PLA positive spots were observed in intestinal sections of CIP2A^{HOZ} mice (Figure 4E and F).

CIP2A is dispensable for normal intestinal crypt homeostasis but promotes intestinal regeneration in response to DNA damage

MYC is essential for normal crypt structure in the adult intestine (Muncan et al., 2006; Soucek et al., 2008). On the other hand, recent analyses demonstrated normal growth, weight, development and life-span of CIP2A^{HOZ} mice despite lack of CIP2A expression in all studied organs (Laine et al., 2013; Ventela et al., 2012). This suggests that protein interaction between CIP2A and MYC in intestinal cells may not be essential for intestinal crypt homeostasis. In line with this hypothesis, comparison of BrdU positivity and number of paneth and goblet cells in the intestines of WT and CIP2A^{HOZ} did not reveal any indications of disturbance in proliferation or differentiation of intestinal crypts. (Figure S4). Also CIP2A^{HOZ} mice did not reveal any gross changes in the crypt architecture as compared to WT mice (Figure S4). These results demonstrate that CIP2A is dispensable for normal crypt function.

Notably, similar to MYC induction in response to DNA damage (Ashton et al., 2010; Athineos and Sansom, 2010), the regenerating intestinal tissue displayed marked CIP2A upregulation both at the protein and mRNA levels, whereas the CIP2A^{HOZ} intestine remained CIP2A-deficient even under these conditions (Figures 5A and B). To determine if the increased CIP2A expression functionally contributes to MYC-dependent intestinal regeneration, crypt regeneration following irradiation was studied in CIP2A^{HOZ} mice and their wild-type controls. Control intestines demonstrated a robust regenerative response and this response was significantly attenuated in the absence of CIP2A (Figures 5C and D). Additionally, the regenerating crypts that were observed in CIP2A^{HOZ} mice were significantly less proliferative than in control mice (Figures 5E and F), whereas CIP2A loss did not increase apoptosis induction in intestinal crypts acutely after irradiation (Figure 5G). To control that CIP2A-dependency of intestinal regeneration is a general phenomenon related to DNA-damage, the mice were treated systemically with the chemotherapy agent

cisplatin. Importantly, in response to cisplatin treatment, CIP2A^{HOZ} intestines showed an even more dramatic perturbation in the regenerative and proliferative response than in response to irradiation (Figures 5H–J).

To study whether CIP2A is expressed in Lgr5+ intestinal crypt stem celllike cells, we exploited a transgenic mouse model expressing GFP under Lgr5 promoter (Metcalfe et al., 2014). As shown in figure 5K, CIP2A mRNA was relatively more expressed in GFP positive (Lgr5+) cell population than in Lgr5-cells. However, as compared to OLFM4, which is a bona fide intestinal crypt stem cell factor (van der Flier et al., 2009), CIP2A was not enriched to same extent (Figure 6K), which is in accordance with positive CIP2A IHC staining also in other intestinal crypt cells (Figure 4A).

These results demonstrate that CIP2A is promotes MYC-dependent intestinal regeneration induced by DNA damage.

CIP2A is critical for the transcriptional activation of MYC targets during intestinal regeneration

Next, we asked whether the phenotypic outcome in intestinal tissue regeneration in CIP2A^{HOZ} mice is truly linked to the modification of MYC function. First, we investigated MYC expression levels in untreated intestines from control and CIP2A^{HOZ} mice and found no obvious difference (Figure 6A). In addition, upon regeneration, quantification of the intensity of MYC staining per cell within the crypt boundaries (Figure 6B, dashed line and inserts) in 50 consecutive crypts per mouse revealed that MYC immunopositivity in CIP2A^{HOZ} mice within the crypt was at the same level than in WT crypts (Figure 6C). In addition, and similar to MEFs, c-*myc* mRNA was expressed at equal levels between regenerating WT and CIP2A^{HOZ} crypts (Figure 6D). However, fully consistent with our *in vitro* results that CIP2A selectively regulates pS62MYC (Figure 2D and E), irradiation-induced expression of pS62MYC was inhibited in CIP2A^{HOZ} crypts (Figures 6E and F) and this correlated with induction of proliferation assessed by Ki67 co-staining (Figure 6E and 6E,F).

Next, we next performed a qRT-PCR analysis of irradiated wild-type and CIP2A^{HOZ} intestines on a number of MYC target genes involved in intestinal regeneration (Athineos and Sansom, 2010; Sansom et al., 2007). Of the genes analysed, all were significantly downregulated in regenerating guts from CIP2A^{HOZ} mice compared to controls (Figure 6G). We also confirmed impaired MYC recruitment to *tiam1* promoter upon CIP2A inhibition by siRNA in cultured cells (Figure S5). MYC and CIP2A dependence of protein expression for selected MYC target genes was further confirmed using IHC (Figure 6H). Quantification of CDK4 and TIAM1 expression from adjacent sections of those from which MYC expression was quantified (Figure 6B), confirmed the significant inhibition of expression of both of these MYC targets in regenerating CIP2A^{HOZ} intestine (Figure 6I).

Together these results provide *in vivo* validation that CIP2A selectively support expression of serine 62 phosphorylated MYC.

Confirmation of the importance of MYC serine 62 phosphorylation for proliferation induction *in vivo*

To validate our main conclusion that expression of pS62MYC is critical for proliferation induction *in vivo*, we returned to use the MYC serine 62 phosphorylation mutants in *in vivo* setting. We hypothesized that T58A might more potently than wild-type (WT) MYC and S62A MYC rescue the effects of endogenous MYC loss in intestinal regeneration model. We have recently shown that wild-type (WT) *c-myc* ($Rosa^{Myc/+}$) transgene expression at a subphysiological level is unable to drive a regenerative response in the absence of endogenous, Wnt-induced c-*myc* (Ashton et al., 2010).

To this end, we crossed *AhCre* $Myc^{fl/fl}$ mice with mice carrying a *Lox-stop-Lox c-myc, Lox-stop-Lox c-*myc^{T58A}, and *Lox-stop-Lox c-*myc^{S62A} allele to generate $Myc^{fl/fl}$ $Rosa^{Myc/+}$, $Myc^{fl/fl}$ $Rosa^{MycT58A/+}$, and $Myc^{fl/fl}$ $Rosa^{MycS62A/+}$ *mice* respectively (Figure S6A). This cross permits B-napthoflavone-induced expression of either the wild-type (WT), T58A or S62A allele of MYC at subphysiological levels in the absence of endogenous, Wnt-induced c-*myc*. Importantly, upon recombination the transgenes were transcriptionally expressed at the same level (Figure S6B), whereas the both T58AMYC and S62AMYC showed significantly higher protein expression in regenerating intestine than WT MYC (Figure 7A). Increased expression of T58A mutant is presumably due to its higher protein stability, whereas higher protein expression of S62MYC than WT MYC upon tissue regeneration may be due to compensation mechanism as discussed below. However, despite similar protein expression levels of T58AMYC and S62AMYC as assessed by total MYC antibody, MYCT58A mutant did show significantly increased level of serine 62 phosphorylation in regenerating intestine tissue as compared to either S62A of WT MYC (Figure 7B and C). This finding is consistent with previously published data (Lutterbach and Hann, 1994; Sears et al., 2000), and allows comparison of these models to assess whether the form of MYC that drives highest regeneration potential *in vivo* is the serine 62 phosphorylated MYC. Irradiation of WT mice resulted again in a robust regenerative response 72 h later as evidenced by large crypts that stain positively for Ki67 (Figure S6C and 7D). However, the conditional deletion of *c-myc* by IP injection of B-napthoflavone ($Myc^{fl/fl}$) suppressed the regeneration (Figures 7D and Figure S6C). As before (Ashton et al., 2010), the B-naptoflavone injection-elicited expression of WT *c-myc* ($Rosa^{Myc/+}$) at a subphysiological level was unable to drive a regenerative response (Figures 7D and S6C). However, consistent with all other data indicating that serine 62 phosphorylation defines MYC's proliferative potential, T58AMYC was significantly more competent than WT of S62AMYC to compensate for the loss of endogenous *c-myc*, both in regeneration response as well as in driving cell proliferation in response to irradiation (Figures 7D, E and S6C). Importantly, we did not observe any gross histological differences or proliferative effects following the expression of T58AMYC transgene in untreated wild-type mice, indicating that the increased regeneration by T58AMYC was not due to a more proliferative environment (Figure S6D). Furthermore, in full support to our *in vitro* results that the serine 62 phosphorylation is a determinant factor whether MYC interacts with both CIP2A (Junttila et al., 2007) and Lamin A/C (Figure 2A–C), the PLA analysis on regenerating intestinal tissues demonstrate almost absolute lack of LAS localization of MYCS62A, whereas MYCT58A robustly interact with both CIP2A and Lamin A/C *in vivo* (Figure 7F).

Finally, we confirmed that expression of MYCT58A also rescued expression of number of CIP2A-regulated MYC target genes that were downregulated in *Myc*$^{fl/fl}$ intestine (Figure 7G). Importantly among those that were rescued was Tiam1 that was used as a model gene to demonstrate CIP2A's role in MYC promoter recruitment (Figure S5).

Together these results strongly support our main conclusions that the form of MYC protein that drives *in vivo* proliferation and DNA-damage induced regeneration is pS62MYC, and that association of pS62MYC with both LAS and CIP2A is intimately linked to MYC-mediated proliferation induction and gene expression *in vivo*.

DISCUSSION

Development of targeted therapies requires thorough understanding of the molecular mechanisms regulating the target activity, as well as, validation of the importance of this mechanism in a faithful *in vivo* model. Based on extensive research during the past three decades, it has become evident that targeting of MYC would be highly desirable for hyperproliferative diseases (Meyer and Penn, 2008; Soucek et al., 2008). Surprisingly though, until now it has not been demonstrated what endogenous post-translational mechanism defines MYC activity *in vivo*. In this work we demonstrate by using both CIP2A and MYC mouse models that CIP2A-mediated support of MYC serine 62 phosphorylation is critically linked to MYC's capacity to re-initiate proliferation, and support intestinal regeneration in response to DNA damage. Importantly, our data indicate that neither CIP2A, nor MYC serine 62 phosphorylation impacts basal proliferation, or differentiation, of intestinal crypt cells. Therefore, MYC serine 62 phosphorylation appears to be selectively required to support MYC-mediated high-level proliferation. In addition to their biological importance, these results indicate that selective targeting of mechanisms that support serine 62 phosphorylation MYC might constitute a therapy strategy for hyperproliferative diseases. Specifically, the results indicate that targeting the CIP2A could offer a possibility to interfere with MYC-mediated proliferation without detrimental consequences on normal physiology. However, we cannot currently exclude that in addition to MYC, inhibition of other CIP2A-regulated proteins (Khanna et al., 2013; Puustinen et al., 2014) could also partly contribute to *in vivo* effects of CIP2A inhibition in intestinal regeneration. On the other hand the results imply that pharmaceutical inhibition of CIP2A might affect regeneration of normal tissues if combined with DNA-damaging anticancer drugs. Therefore targeting of CIP2A should be combined for example with localized radiotherapy targeting specifically the tumor tissue. In support to importance of CIP2A in mediating radioresistance in human cancers, we have recently published that high expression of tumor CIP2A and stem cell factor Oct4 predicts for poor patient survival among cancer patients treated with radiotherapy (Ventela et al., 2014).

Even though serine 62 phosphorylation regulates MYC stability in cultured cells (Hann, 2006; Sears et al., 2000), our data show that upon irradiation induced proliferation *in vivo*, loss of endogenous MYC serine 62 phosphorylation by CIP2A inhibition does not abrogate total MYC expression (Figure 6B and C). Interestingly, the S62AMYC mutant also did not show significant difference in protein expression as compared to T58AMYC. We speculate that either there is a fundamental difference in role of serine 62 phosphorylation or MYC in

its stability regulation between *in vitro* and *in vivo* context or that upon loss of serine 62 phosphorylation *in vivo*, intestinal cells under DNA-damage induced stress compensate the situation by increasing expression of MYC that is not phosphorylated on serine 62, by some yet unknown mechanism. We cannot also exclude that the non-significantly decreased median expression of S62AMYC may in part contribute to proliferation defect, caused by loss of serine 62 phosphorylation. We also note some focal positive staining with pS62MYC antibody in the nucleus of even MYCfl/fl mice and this can be due to compensatory expression of NMYC as the sequences surrounding S62 are nearly 100% conserved between MYC and NMYC.

Importantly, the cell culture experiments revealed a plausible explanation for the selectivity of CIP2A towards pS62MYC. We show that serine 62 phosphorylation promotes MYC recruitment to LAS and that only the pS62MYC that is associated with LAS is sensitive to regulation by CIP2A, whereas MYC in soluble nuclear fraction was resistant to CIP2A depletion. Importantly, the preferential association of T58AMYC, exhibiting increased serine 62 phosphorylation, with LAS and CIP2A was validated *in* vivo (Figure 7F). Most importantly, functional outcomes of both $CIP2A^{HOZ}$ and S62AMYC models perfectly support the overall conclusions of this work that when MYC is phosphorylated on serine 62, it interacts with both LAS and CIP2A, and that this biochemical form of MYC drives in vivo proliferation and regeneration.

Consistent with an emerging picture of nuclear lamin-associated domains as critical structures for gene regulation and chromatin remodelling (Kind et al., 2013; Shimi et al., 2010; Zullo et al., 2012), our data indicate that CIP2A-MYC interaction at LAS is essential for maintaining transcription-competent MYC that subsequently binds to its target promoters to promote expression of proliferation inducing genes. Importantly, recent studies have also indicated that serine 62 phosphorylation of MYC may affect target promoter selection (Benassi et al., 2006; Farrell et al., 2013), which is another interesting aspect to study in future by using CIP2A-deficient mouse model. Also, association of CIP2A with nuclear pores (data not shown)(Thakar et al., 2012) is consistent with recent indication that multiprotein platforms at nuclear pores are key regulators of DNA damage response (Arib and Akhtar, 2011; Bukata et al., 2013). Of historical note, association of MYC with the nuclear envelope has been demonstrated previously (Eisenman et al., 1985; Winqvist et al., 1984), and MYC stability has been linked to its subnuclear partioning (Tworkowski et al., 2002), but the physiological relevance of these findings has been obscure thus far.

In summary, these results demonstrate that MYC serine 62 phosphorylation is a non-essential mechanism that supports MYC's proliferative activity *in vivo*. As CIP2A supports pS62MYC expression and other oncogenic driver phosphorylation events (Khanna et al., 2013), but is non-essential in normal physiology, development of chemical inhibitors of CIP2A is a prospective approach for inhibition of proliferation *in vivo* without therapy-limiting side-effects. We also envision that our results will provoke future studies to identify other therapeutic strategies to inhibit MYC serine 62 phosphorylation. Moreover, our demonstration that transcription factor function and accumulation is regulated at LAS suggest the potential for targeting these structures for future therapies. Finally, our data demonstrate CIP2A as a signalling protein that is indispensable for efficient recovery and

regeneration of intestinal tissue in response to DNA-damage, implying an important role for CIP2A in organismal DNA-damage response.

EXPERIMENTAL PROCEDURES

Mouse experiments

All experiments were performed under the UK Home Office guidelines. All mice used were of a mixed background (50% C57BlJ, 50% S129). The alleles used for this study were as follows: *c-Myc*^{fl} (de Alboran et al., 2001), *AhCre* (Ireland et al., 2004), *Rosa*^{Myc} (Wang et al., 2011), *Rosa*^{MycT58} (Wang et al., 2011), *CIP2A*^{HOZ} (Ventela et al., 2012). To determine the role of Myc protein stability during intestinal regeneration *AhCre c-Myc*$^{fl/fl}$ mice were crossed to *Rosa*^{Myc}, *Rosa*^{MycT58A}, or *Rosa*^{MycS62A} mice. Control, *AhCre c-Myc*$^{fl/fl}$, *AhCre c-Myc*$^{fl/fl}$ *Rosa*$^{Myc/+}$, *AhCre c-Myc*$^{fl/fl}$ *Rosa*$^{MycT58A/+}$ or *AhCre c-Myc*$^{fl/fl}$ *Rosa*$^{MycS62A/+}$ mice were given 3 intraperitoneal (IP) injections of 80mg/kg-β-napthoflavone in a single day, which yields nearly constitutive recombination in the murine small intestine. Intestinal regeneration experiments have been described previously (Myant et al., 2013), and the protocol is included in the supplementary experimental procedures.

Immunohistochemistry

Standard immunohistochemistry techniques were used throughout this study. Primary antibodies used for immunohistochemistry were as follows: Ki67 (Vector VP-K452), c-Myc (Santa Cruz sc-764), BrdUrd (BD Biosciences), CDK4 (Santa Cruz sc-260), Tiam1 (Santa Cruz sc-872), CIP2A (Junttila et al., 2007; Laine et al., 2013; Soo Hoo et al., 2002; Ventela et al., 2012), and pS62MYC(Junttila et al., 2007; Wang et al., 2011; Yeh et al., 2004). Immunohistochemistry was performed on formalin-fixed intestinal sections. For each antibody, staining was performed on at least 3 mice of each genotype. For histoscoring, the average staining intensity in 50 consecutive crypts was scored from at least 6 mice. For MYC serine 62 phosphorylation the fluorescent signal for pS62MYC intensity and DAPI intensity were calculated from four slides each representing different treatment/phenotype. From these 10 pictures/each slide was taken and from each picture, nucleus staining was quantified by drawing a circle around 20 nuclei using the OpenLab 5.5 software and the signal intensity was measured from 50 nuclei/crypt from each picture using IMAGE-J. MYC phosphorylation status is expressed as pS62MYC/DAPI ratio using the average of the intensity from all measurements per treatment/genotype. The error bar represents the averaged intensity calculated in 4 mice. Similar results were obtained from two independent series of experiments performed one year apart from each other. Representative images are shown for each staining. Scale bar in all figures is 50 um.

Proximity ligation assay and immunofluorescence stainings

The PLA assay was performed according to manufacturer protocol (Olink Bioscience). Briefly, cells plated on coverslips were grown to 70% confluence, fixed with 3:1 acetone methanole in −20°C for 5–7 min, and blocked with blocking solution, incubated in a pre-heated humidity chamber for 30 minutes at 37°C, followed by incubating primary antibodies (in blocking solution) anti-CIP2A (Soo Hoo et al., 2002), anti-CIP2A (sc-80659, Santa Cruz), anti-MYC (9E10, Sigma), anti-Lamin A/C (goat, sc-6215, Santa Cruz), anti-LAP2

(611000, BD Transduction Laboratories), anti-Lamin A/C (636, mouse, sc-7292, Santa Cruz), anti-Lamin A/C (H-110, rabbit, sc-20681, Santa Cruz), anti-c-Myc (phospho S62) (mouse, ab78318, abcam), overnight at 4°C. Subsequently, cells were washed with Buffer A, and PLA probe was incubated in a pre-heated humidity chamber for 1h at 37°C followed by ligase reaction in a pre-heated humidity chamber for 1h at 37°C. Next, Amplification-Polymerase solution for PLA, and the secondary antibody Alexa Fluor® 488 (Invitrogen) for Lamin A/C (goat, sc-6215, Santa Cruz) used for CIP2A-MYC and CIP2A-pS62MYC PLA were added, followed by incubating cells in a pre-heated humidity chamber for 100 minutes at 37°C.

For tissue samples, formalin-fixed slides were dewaxed in xylene, and then rehydrated in decreasing concentrations of alcohol, followed by washing two times in tap water. The slides were then incubated in antigen-retrieval buffer (Lab Vision citrate buffer, Thermo Scientific) for 30 min at 99°C, followed by cooling down to room temperature and rinsing slides in dH2O. Next, the slides were blocked for 15 minutes in 1.5% H2O2 solution in PBS, followed by rising in dH2O and once in TBST buffer. Finally, the PLA assay was performed following the PLA protocol for cell staining from blocking slides by blocking solution. Immunofluorescence for CIP2A, MYC (sc-764, Santa Cruz), pS62MYC (ab51156, abcam) and Lamin A/C (sc-7292, Santa Cruz) was performed as described previously (Junttila et al., 2007). All fluorescent stainings were analyzed by confocal microscope LSM780 (Carl Zeiss).

Supplementary Material

Refer to Web version on PubMed Central for supplementary material.

ACKNOWLEDGEMENTS

The authors thank Prof. Martin Eilers, Prof. Johanna Ivaska, Dr. Pekka Taimen and Dr. Daniel Abankwa for critical reading of the manuscript and Prof. Bruno Amati for his valuable advice regarding ChIP analysis. Taina Kalevo-Mattila is thanked for technical help and Jouko Sandström and Markku Saari at Turku Centre for Biotechnology Cell Imaging Core facility for help in imaging. This study was supported by funding from Association of International Cancer Research (grants 08-0614 and 10-0643), Academy of Finland (grants 122546, 137687 and 267817), Finnish Cancer Organisations, Foundation of Finnish Cancer Institute, Sigrid Juselius Foundation, NIH (R01 CA129040 and R01 CA100855), European research council (Coloncan), European Commission FP7- Health (278568), and Cancer Research UK (A12481).

REFERENCES

Arib G, Akhtar A. Multiple facets of nuclear periphery in gene expression control. Curr Opin Cell Biol. 2011; 23:346–353. [PubMed: 21242077]

Ashton GH, Morton JP, Myant K, Phesse TJ, Ridgway RA, Marsh V, Wilkins JA, Athineos D, Muncan V, Kemp R, et al. Focal adhesion kinase is required for intestinal regeneration and tumorigenesis downstream of Wnt/c-Myc signaling. Dev Cell. 2010; 19:259–269. [PubMed: 20708588]

Athineos D, Sansom OJ. Myc heterozygosity attenuates the phenotypes of APC deficiency in the small intestine. Oncogene. 2010; 29:2585–2590. [PubMed: 20140021]

Benassi B, Fanciulli M, Fiorentino F, Porrello A, Chiorino G, Loda M, Zupi G, Biroccio A. c-Myc phosphorylation is required for cellular response to oxidative stress. Mol Cell. 2006; 21:509–519. [PubMed: 16483932]

Bukata L, Parker SL, D'Angelo MA. Nuclear pore complexes in the maintenance of genome integrity. Curr Opin Cell Biol. 2013; 25:378–386. [PubMed: 23567027]

Capelson M, Doucet C, Hetzer MW. Nuclear pore complexes: guardians of the nuclear genome. Cold Spring Harbor symposia on quantitative biology. 2010; 75:585–597. [PubMed: 21502404]

de Alboran IM, O'Hagan RC, Gartner F, Malynn B, Davidson L, Rickert R, Rajewsky K, DePinho RA, Alt FW. Analysis of C-MYC function in normal cells via conditional gene-targeted mutation. Immunity. 2001; 14:45–55. [PubMed: 11163229]

Dechat T, Adam SA, Taimen P, Shimi T, Goldman RD. Nuclear lamins. Cold Spring Harbor perspectives in biology. 2010; 2:a000547. [PubMed: 20826548]

Dubois NC, Adolphe C, Ehninger A, Wang RA, Robertson EJ, Trumpp A. Placental rescue reveals a sole requirement for c-Myc in embryonic erythroblast survival and hematopoietic stem cell function. Development. 2008; 135:2455–2465. [PubMed: 18550708]

Eisenman RN, Tachibana CY, Abrams HD, Hann SR. V-myc- and c-myc-encoded proteins are associated with the nuclear matrix. Mol Cell Biol. 1985; 5:114–126. [PubMed: 3872410]

Farrell AS, Pelz C, Wang X, Daniel CJ, Wang Z, Su Y, Janghorban M, Zhang X, Morgan C, Impey S, et al. Pin1 regulates the dynamics of c-Myc DNA binding to facilitate target gene regulation and oncogenesis. Mol Cell Biol. 2013; 33:2930–2949. [PubMed: 23716601]

Finch AJ, Soucek L, Junttila MR, Swigart LB, Evan GI. Acute overexpression of Myc in intestinal epithelium recapitulates some but not all the changes elicited by Wnt/beta-catenin pathway activation. Mol Cell Biol. 2009; 29:5306–5315. [PubMed: 19635809]

Hann SR. Role of post-translational modifications in regulating c-Myc proteolysis, transcriptional activity and biological function. Semin Cancer Biol. 2006; 16:288–302. [PubMed: 16938463]

Ireland H, Kemp R, Houghton C, Howard L, Clarke AR, Sansom OJ, Winton DJ. Inducible Cre-mediated control of gene expression in the murine gastrointestinal tract: effect of loss of beta-catenin. Gastroenterology. 2004; 126:1236–1246. [PubMed: 15131783]

Janssens V, Goris J. Protein phosphatase 2A: a highly regulated family of serine/threonine phosphatases implicated in cell growth and signalling. Biochem J. 2001; 353:417–439. [PubMed: 11171037]

Junttila MR, Puustinen P, Niemela M, Ahola R, Arnold H, Bottzauw T, Ala-aho R, Nielsen C, Ivaska J, Taya Y, et al. CIP2A inhibits PP2A in human malignancies. Cell. 2007; 130:51–62. [PubMed: 17632056]

Khanna A, Pimanda JE, Westermarck J. Cancerous inhibitor of protein phosphatase 2A, an emerging human oncoprotein and a potential cancer therapy target. Cancer Res. 2013; 73:6548–6553. [PubMed: 24204027]

Kim JS, Kim EJ, Oh JS, Park IC, Hwang SG. CIP2A modulates cell cycle progression in human cancer cells by regulating the stability and activity of PLK1. Cancer Res. 2013

Kind J, Pagie L, Ortabozkoyun H, Boyle S, de Vries SS, Janssen H, Amendola M, Nolen LD, Bickmore WA, van Steensel B. Single-cell dynamics of genome-nuclear lamina interactions. Cell. 2013; 153:178–192. [PubMed: 23523135]

Laine A, Sihto H, Come C, Rosenfeldt MT, Zwolinska A, Niemela M, Khanna A, Chan EK, Kahari VM, Kellokumpu-Lehtinen PL, et al. Senescence Sensitivity of Breast Cancer Cells Is Defined by Positive Feedback Loop between CIP2A and E2F1. Cancer discovery. 2013; 3:182–197. [PubMed: 23306062]

Luscher B, Vervoorts J. Regulation of gene transcription by the oncoprotein MYC. Gene. 2012; 494:145–160. [PubMed: 22227497]

Lutterbach B, Hann SR. Hierarchical phosphorylation at N-terminal transformation-sensitive sites in c-Myc protein is regulated by mitogens and in mitosis. Mol Cell Biol. 1994; 14:5510–5522. [PubMed: 8035827]

Mateyak MK, Obaya AJ, Adachi S, Sedivy JM. Phenotypes of c-Myc-deficient rat fibroblasts isolated by targeted homologous recombination. Cell growth & differentiation : the molecular biology journal of the American Association for Cancer Research. 1997; 8:1039–1048. [PubMed: 9342182]

Metcalfe C, Kljavin NM, Ybarra R, de Sauvage FJ. Lgr5+ Stem Cells Are Indispensable for Radiation-Induced Intestinal Regeneration. Cell stem cell. 2014; 14:149–159. [PubMed: 24332836]

Meyer N, Penn LZ. Reflecting on 25 years with MYC. Nat Rev Cancer. 2008; 8:976–990. [PubMed: 19029958]

Muncan V, Sansom OJ, Tertoolen L, Phesse TJ, Begthel H, Sancho E, Cole AM, Gregorieff A, de Alboran IM, Clevers H, et al. Rapid loss of intestinal crypts upon conditional deletion of the Wnt/Tcf-4 target gene c-Myc. Mol Cell Biol. 2006; 26:8418–8426. [PubMed: 16954380]

Myant KB, Cammareri P, McGhee EJ, Ridgway RA, Huels DJ, Cordero JB, Schwitalla S, Kalna G, Ogg EL, Athineos D, et al. ROS production and NF-kappaB activation triggered by RAC1 facilitate WNT-driven intestinal stem cell proliferation and colorectal cancer initiation. Cell stem cell. 2013; 12:761–773. [PubMed: 23665120]

Niemelä M, Kauko O, Sihto H, Mpindi JP, Nicorici D, Pernilä P, Kallioniemi OP, Joensuu H, Hautaniemi S, Westermarck J. CIP2A signature reveals the MYC dependency of CIP2A-regulated phenotypes and its clinical association with breast cancer subtypes. Oncogene. 2012; 31:4266–4278. [PubMed: 22249265]

Nieminen AI, Partanen JI, Hau A, Klefstrom J. c-Myc primed mitochondria determine cellular sensitivity to TRAIL-induced apoptosis. EMBO J. 2007; 26:1055–1067. [PubMed: 17268552]

Perna D, Faga G, Verrecchia A, Gorski MM, Barozzi I, Narang V, Khng J, Lim KC, Sung WK, Sanges R, et al. Genome-wide mapping of Myc binding and gene regulation in serum-stimulated fibroblasts. Oncogene. 2012; 31:1695–1709. [PubMed: 21860422]

Puustinen P, Rytter A, Mortensen M, Kohonen P, Moreira JM, Jaattela M. CIP2A oncoprotein controls cell growth and autophagy through mTORC1 activation. J Cell Biol. 2014; 204:713–727. [PubMed: 24590173]

Sansom OJ, Meniel VS, Muncan V, Phesse TJ, Wilkins JA, Reed KR, Vass JK, Athineos D, Clevers H, Clarke AR. Myc deletion rescues Apc deficiency in the small intestine. Nature. 2007; 446:676–679. [PubMed: 17377531]

Sears R, Leone G, DeGregori J, Nevins JR. Ras enhances Myc protein stability. Mol Cell. 1999; 3:169–179. [PubMed: 10078200]

Sears R, Nuckolls F, Haura E, Taya Y, Tamai K, Nevins JR. Multiple Ras-dependent phosphorylation pathways regulate Myc protein stability. Genes Dev. 2000; 14:2501–2514. [PubMed: 11018017]

Shimi T, Butin-Israeli V, Adam SA, Goldman RD. Nuclear lamins in cell regulation and disease. Cold Spring Harbor symposia on quantitative biology. 2010; 75:525–531. [PubMed: 21467145]

Soo Hoo L, Zhang JY, Chan EK. Cloning and characterization of a novel 90 kDa 'companion' auto-antigen of p62 overexpressed in cancer. Oncogene. 2002; 21:5006–5015. [PubMed: 12118381]

Soucek L, Whitfield J, Martins CP, Finch AJ, Murphy DJ, Sodir NM, Karnezis AN, Swigart LB, Nasi S, Evan GI. Modelling Myc inhibition as a cancer therapy. Nature. 2008; 455:679–683. [PubMed: 18716624]

Thakar K, Karaca S, Port SA, Urlaub H, Kehlenbach RH. Identification of CRM1-dependent nuclear export cargos using quantitative mass spectrometry. Mol Cell Proteomics. 2012

Thomas LR, Tansey WP. Proteolytic control of the oncoprotein transcription factor Myc. Adv Cancer Res. 2011; 110:77–106. [PubMed: 21704229]

Trumpp A, Refaeli Y, Oskarsson T, Gasser S, Murphy M, Martin GR, Bishop JM. c-Myc regulates mammalian body size by controlling cell number but not cell size. Nature. 2001; 414:768–773. [PubMed: 11742404]

Tworkowski KA, Salghetti SE, Tansey WP. Stable and unstable pools of Myc protein exist in human cells. Oncogene. 2002; 21:8515–8520. [PubMed: 12466972]

van der Flier LG, Haegebarth A, Stange DE, van de Wetering M, Clevers H. OLFM4 is a robust marker for stem cells in human intestine and marks a subset of colorectal cancer cells. Gastroenterology. 2009; 137:15–17. [PubMed: 19450592]

Ventela S, Come C, Makela JA, Hobbs RM, Mannermaa L, Kallajoki M, Chan EK, Pandolfi PP, Toppari J, Westermarck J. CIP2A promotes proliferation of spermatogonial progenitor cells and spermatogenesis in mice. PLoS ONE. 2012; 7:e33209. [PubMed: 22461891]

Ventela S, Sittig E, Mannermaa L, Makela JA, Kulmala J, Loyttyniemi E, Strauss L, Carpen O, Toppari J, Grenman R, et al. CIP2A is an Oct4 target gene involved in head and neck squamous cell cancer oncogenicity and radioresistance. Oncotarget. 2014

Wang X, Cunningham M, Zhang X, Tokarz S, Laraway B, Troxell M, Sears RC. Phosphorylation Regulates c-Myc's Oncogenic Activity in the Mammary Gland. Cancer Res. 2011; 71:925–936. [PubMed: 21266350]

Winqvist R, Saksela K, Alitalo K. The myc proteins are not associated with chromatin in mitotic cells. EMBO J. 1984; 3:2947–2950. [PubMed: 6396084]

Yeh E, Cunningham M, Arnold H, Chasse D, Monteith T, Ivaldi G, Hahn WC, Stukenberg PT, Shenolikar S, Uchida T, et al. A signaling pathway controlling c-Myc degradation that impacts oncogenic transformation of human cells. Nat Cell Biol. 2004; 6:308–318. [PubMed: 15048125]

Zullo JM, Demarco IA, Pique-Regi R, Gaffney DJ, Epstein CB, Spooner CJ, Luperchio TR, Bernstein BE, Pritchard JK, Reddy KL, et al. DNA sequence-dependent compartmentalization and silencing of chromatin at the nuclear lamina. Cell. 2012; 149:1474–1487. [PubMed: 22726435]

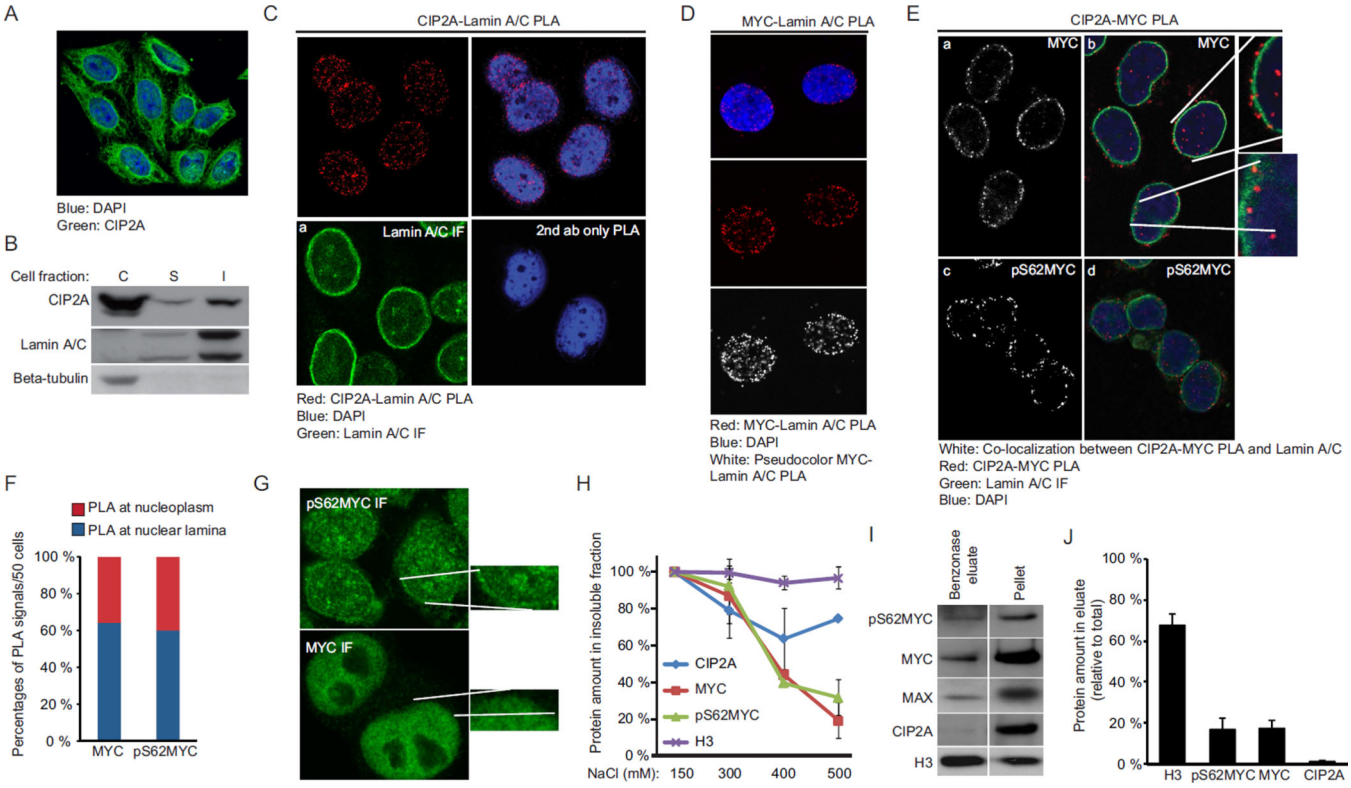

Figure 1. CIP2A and serine 62 phosphorylated MYC interact at Lamin A/C associated proteinaceous nuclear structures

(A) Immunofluorescent staining of CIP2A in Hela cells. (B) Analysis of subcellular distribution of CIP2A in cytoplasmic (C) soluble nuclear (S) and insoluble nuclear (I) fractions of Hela cells by high salt (400 mM NaCl) nuclear extraction. Lamin A/C and Beta-tubulin represent nuclear and cytoplasmic markers, respectively. (C) PLA analysis of CIP2A-Lamin A/C association in Hela cells. Specificity of PLA is shown by lack of PLA signals in secondary antibody only control panel. Panel (a) shows immunofluoresence analysis of Lamin A/C distribution both in nuclear lamina as well as in nucleoplasm. (D) PLA analysis of MYC-Lamin A/C association in Hela cells. White dots are pseudocolor MYC-Lamin A/C PLA signals. (E) PLA analysis of CIP2A-MYC and CIP2A-pS62MYC association in Hela cells. Panels (a, b) and (c, d) show co-localization of CIP2A-MYC and CIP2A-pS62MYC PLA signals with Lamin A/C (white dots). Inserts in panel b show detailed image of association of CIP2A-MYC PLA signal with Lamin A/C. (F) Quantitation of CIP2A-MYC and CIP2A-pS62MYC PLA signals at the nuclear lamina and nucleoplasm from (E)(panels b and d). (G) Immunofluoresence analysis of pS62MYC and total MYC nuclear distribution. Inserts high-light the difference in staining pattern between pS62MYC and MYC. (H) Quantification of relative expression of indicated proteins in insoluble fraction of Hela cells subjected to salt extraction fractionation with increasing NaCl concentrations. (I) Analysis of DNA dependency of CIP2A, pS62MYC and MYC association with insoluble nuclear fraction. Histone H3 was used as control for efficacy of elution of DNA bound proteins. (J) Quantitation of protein amount in Benzonase eluate relative to total amount from panel (I). The samples were loaded on the same gel. Error bar represents S.E.M (n=3).

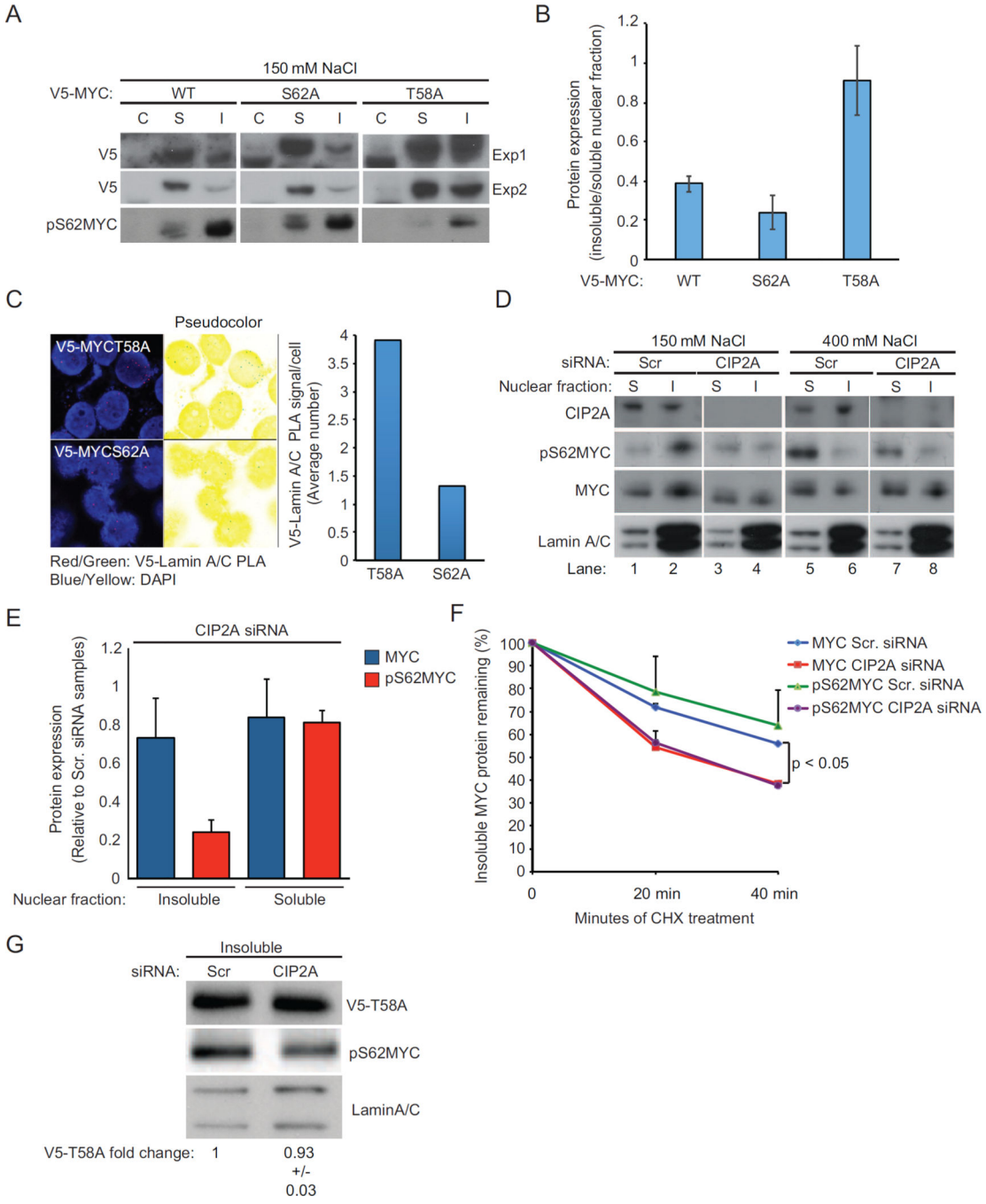

Figure 2. Serine 62 phosphorylation of MYC enhances its recruitment to Lamin A/C-associated nuclear structures and CIP2A is required for retaining this localization

(A) Western blot analysis of subnuclear distribution of exogenous V5-tagged WT, S62A, and T58A MYC and pS62MYC in Hela cells. The fractionation was done with 150mM NaCl. V5 antibody was used to detect WT MYC and S62A, T58A MYC mutants. C, S and I represent cytosolic fraction, soluble nuclear fraction and insoluble nuclear fraction respectively. (B) Quantitation of the ratio of V5-MYC between insoluble and soluble nuclear fractions from (A). Shown is average +/− S.E.M. of two experiments. (C) PLA analysis of V5-Lamin A/C association in Hela cells transfected with equivalent amounts of

V5-MYCT58A or V5-MYCS62A mutant. Shown is quantification of average number of V5-Lamin A/C PLA signal per cell from 50 cells. (D) Analysis of subnuclear portioning of pS62MYC and total MYC in CIP2A siRNA transfected Hela cells. S and I represent soluble nuclear fraction and insoluble nuclear fraction, respectively. Indicated salt extraction conditions were used to either retain (150 mM) or dissociate (400 mM) MYC from insoluble fraction. (E) CIP2A depletion selectively affects pS62MYC localized to insoluble fraction. As lanes 5 and 7 represent proteins that have been extracted from insoluble fraction, the values for the effect of CIP2A depletion on pS62MYC and MYC expression in insoluble fraction represent comparison of lanes 2 and 5 for scrambled siRNA, and 4 and 7 for CIP2A siRNA. Expression of MYC and pS62MYC in soluble fraction was quantified between lanes 1 and 3. Shown is average + S.E.M of two experiments. (F) Effect of CIP2A siRNA on endogenous pS62MYC stability in insoluble nuclear fraction. Symbols denote the average pS62MYC and MYC expression levels at the indicated time points, as compared with non–CHX treated cells. Shown is mean +S.E.M from three independent experiments. (G) Western blot analysis of expression of V5-tagged MYCT58A in insoluble fraction in either scrambled or CIP2A siRNA transfected Hela cells. Endogenous pS62MYC is shown as a control for functional perturbation of CIP2A function, and Lamin A/C was used as a loading control.

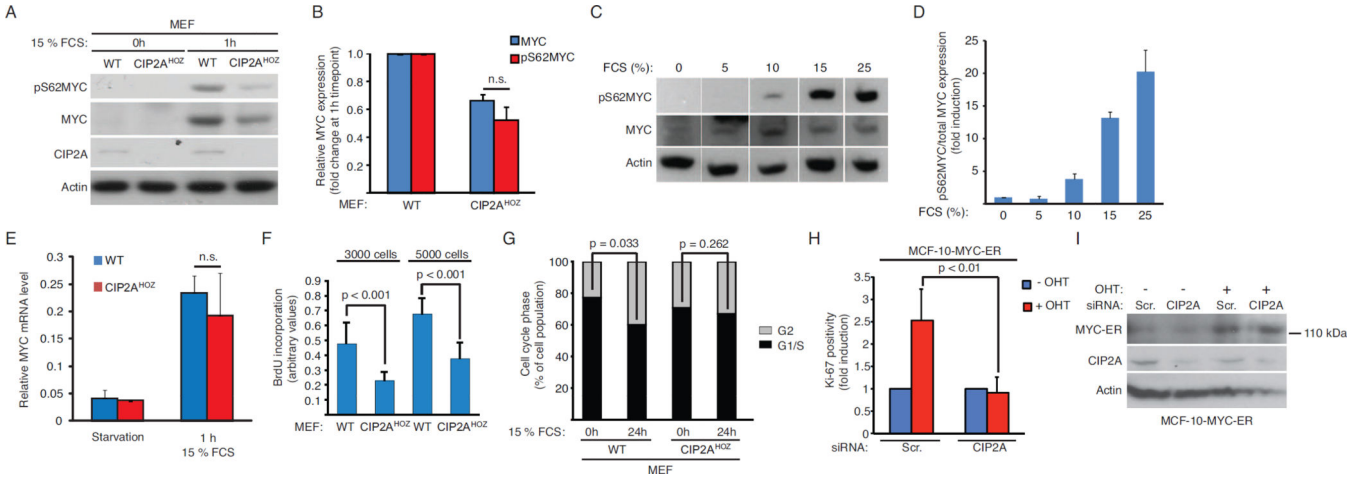

Figure 3. CIP2A is a critical endogenous regulator of MYC phosphorylation and function during proliferation induction

(A) Western blot analysis of pS62MYC, MYC and CIP2A expression in serum starved (0h) and serum stimulated (1h) WT and CIP2A^{HOZ} MEFs. Shown is a representative result of 4 independent experiments with similar results. (B) Quantitation of MYC and pS62MYC protein levels in response to serum induction and normalized to β-actin. Shown is mean +S.E.M. of 4 experiments. n.s = not significant, TTest. (C,D) Analysis of induction of pS62MYC protein expression compared to total MYC in wild type MEFs treated with increasing concentrations of serum. Shown is mean+S.E.M. of 3 experiments. (E) RT-PCR analysis of MYC mRNA expression in serum starved (0h) and serum stimulated (1h) WT and CIP2A^{HOZ} MEFs. Shown is mean + S.D. of two independent experiments. n.s = not significant, TTest. (F) BrdU incorporation of WT and CIP2A^{HOZ} MEFs 48 hours after seeding either 3000 or 5000 cells/well. Shown is mean+SD of 3 independent experiments. TTest. (G) Cell cycle analysis of serum starved (0h) and serum stimulated (24h) WT and CIP2A^{HOZ} MEFs. Shown is percentage of cells in either G1/S or G2 phase. Shown are mean values from three independent experiments. TTest. (H) Induction of proliferation in MCF-10A-MYC-ER cells transfected with CIP2A or control siRNA (Scr.) between OHT treated cells (MYC active) and or control cells (−OHT). Shown is mean + SD of induction of Ki-67 positive cells from three independent experiments. TTest. (I) Western blot analysis of MYC-ER fusion protein (molecular weight 110 kDa) expression in MCF-10A-MYC-ER cells transfected with CIP2A or control siRNA (Scr.)

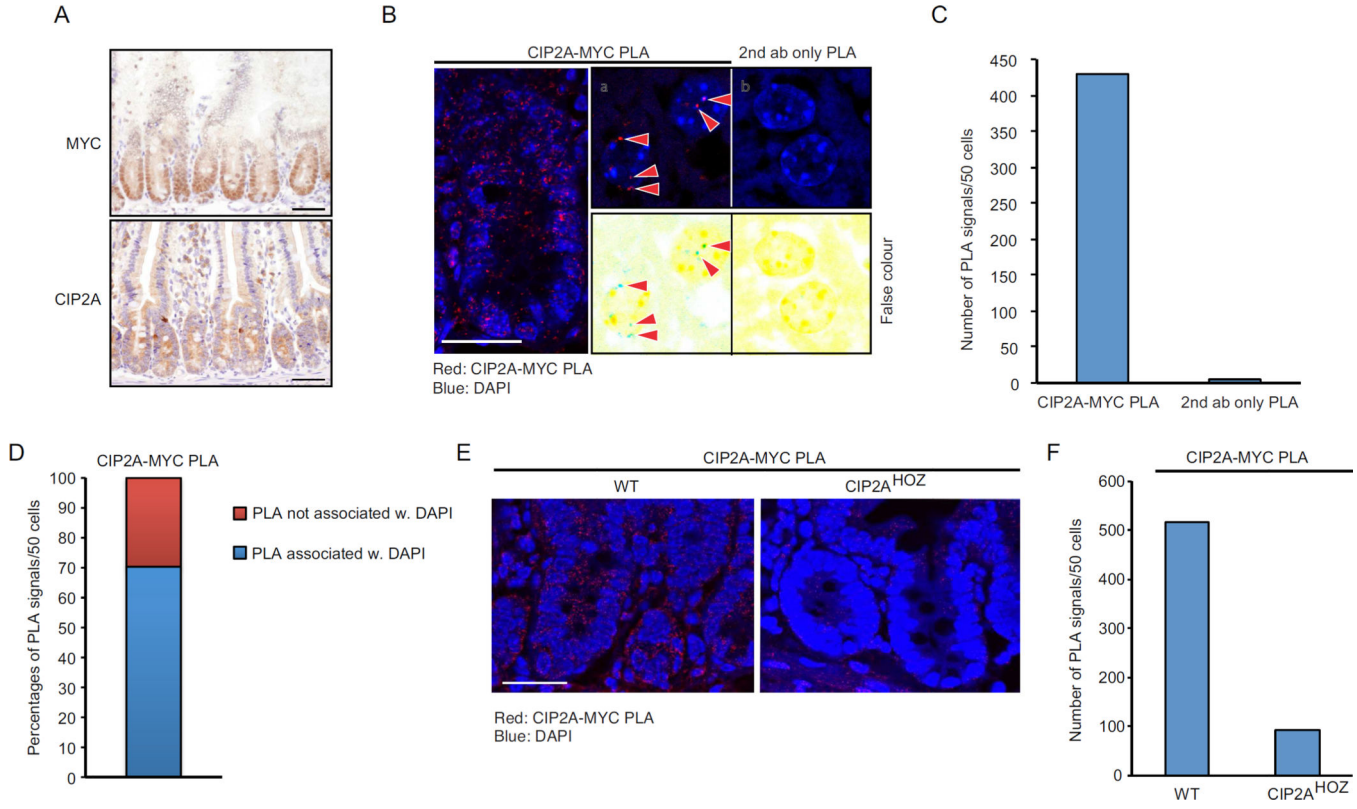

Figure 4. CIP2A interacts with MYC in intestinal tissue

(A) Immunohistochemical staining of endogenous MYC (top panel) and CIP2A (bottom panel) expression in intestinal tissue. Scale bars are 50 μm. (B) CIP2A and MYC physically associate in intestinal cells. Left panel: Red dots indicate association of CIP2A and MYC proteins in intestinal tissue as analysed by Proximity Ligation Assay (PLA). Scale bar is 25 μm. Insert a: red arrowheads indicate positive PLA signals in intestinal cell nuclei. Insert b: no PLA signals were detected by using secondary antibodies (2nd ab) only. (C) Quantitation of number of PLA signals in 50 intestinal cells analysed from panel (B). (D) Quantitation of PLA signals that were associated with nuclear DAPI staining from panel (B). (E) PLA analysis of CIP2A-MYC association in WT and CIP2A^{HOZ} mouse intestinal tissues. Scale bar is 25 μm. (F) Quantitation of number of PLA signals in 50 intestinal cells analysed from panel (E).

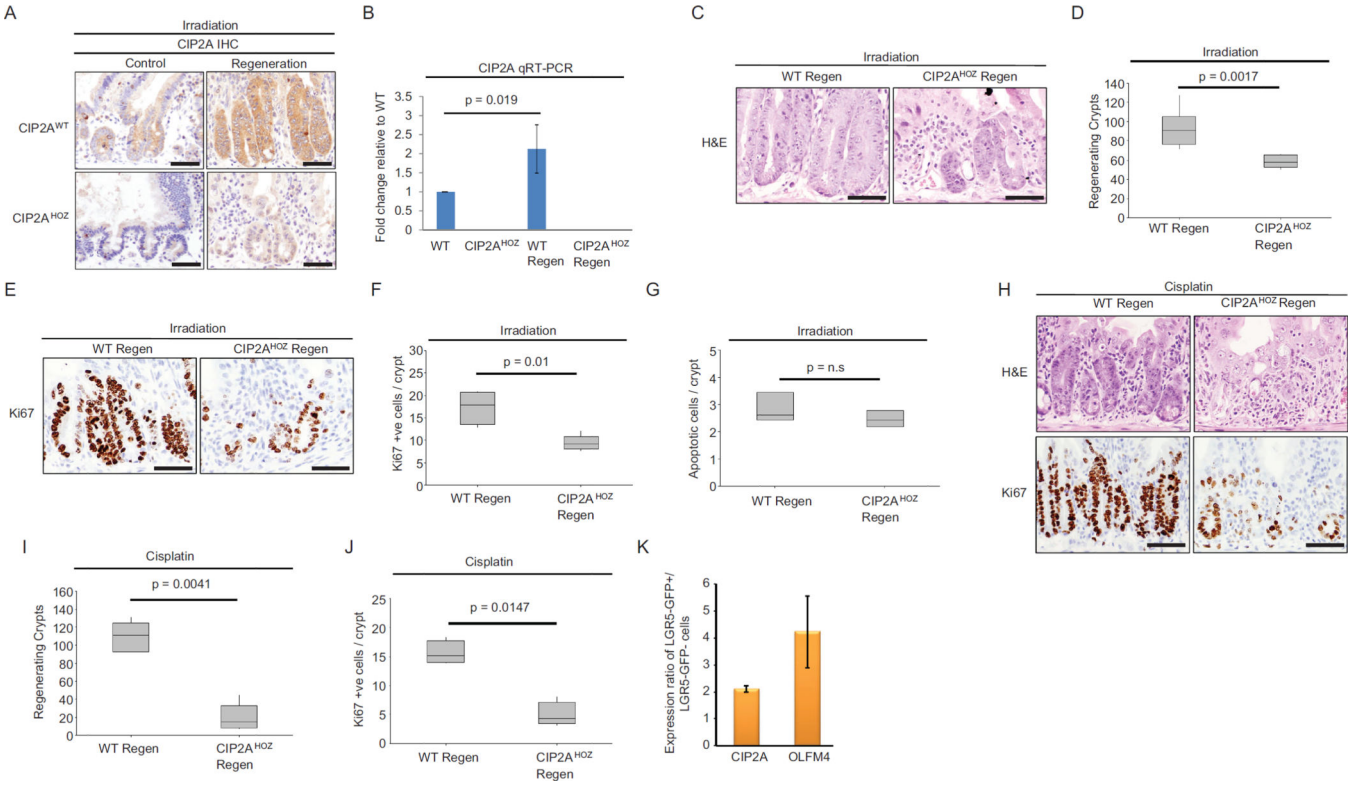

Figure 5. CIP2A promotes intestinal regeneration in response to DNA damage

(A) Immunohistochemical staining of CIP2A in control and regenerating small intestines. Tissue from CIP2A deficient (*CIP2A*^{HOZ}) mice was used to control for antibody specificity (bottom panels). Scale bars are 50 μm. (B) qRT-PCR analysis for CIP2A in WT, *CIP2A*^{HOZ}, WT regenerating and *CIP2A*^{HOZ} regenerating small intestine (TTest, n=3). (C) H&E staining of regenerating crypts from WT and *CIP2A*^{HOZ} intestines following irradiation. Scale bars are 50 μm. (D) Scoring of number of regenerating crypts in WT and *CIP2A*^{HOZ} intestines following irradiation (Mann Whitney, n=7 vs 6). (E) Ki67 staining of regenerating crypts from WT and *CIP2A*^{HOZ} intestines following irradiation. Scale bars are 50 μm. (F) Scoring of number of Ki67 positive cells per crypt in WT and *CIP2A*^{HOZ} intestines following irradiation (Mann Whitney, n=4 vs 5). (G) CIP2A loss does not affect intestinal apoptotic response following DNA damage. Scoring of number of apoptotic cells per crypt in WT and CIP2A^{HOZ} intestines 6h post irradiation. (H) H&E and Ki67 staining of regenerating crypts from WT and *CIP2A*^{HOZ} intestines following cisplatin treatment. Scale bars are 50 μm. (I) Scoring of number of regenerating crypts in WT and *CIP2A*^{HOZ} intestines following cisplatin treatment (Mann Whitney, n=6 vs 5). (J) Scoring of number of Ki67 positive cells per crypt in WT and *CIP2A*^{HOZ} intestines following cisplatin treatment (Mann Whitney, n=4). (K) Expression ratio of CIP2A and OLFM4 mRNA in GFP-LGR5 positive / LGR5 negative intestinal crypt cells after GFP positive cell sorting.

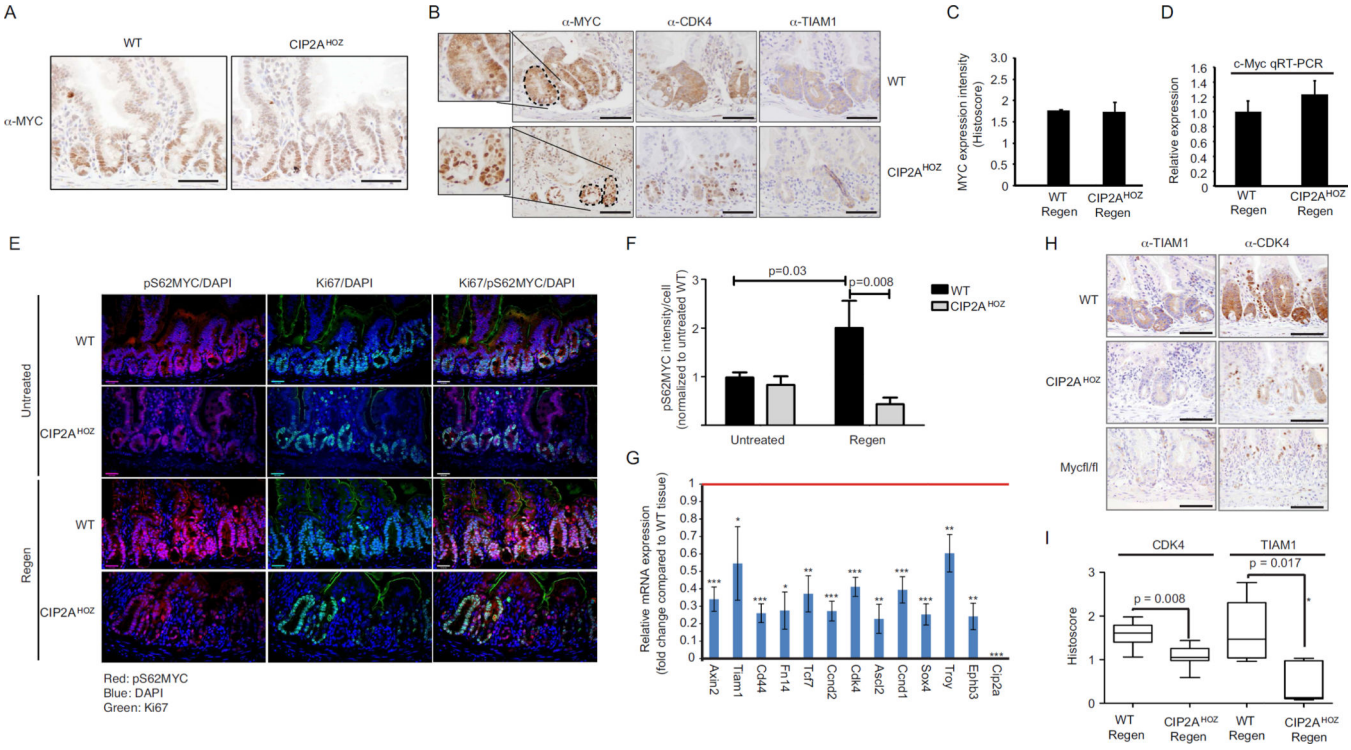

Figure 6. CIP2A is critical for expression of serine 62 phosphorylated MYC and for MYC-driven transcriptional activity during *in vivo* proliferation induction

(A) Immunohistochemical staining of MYC from untreated WT and *CIP2A*^{HOZ} intestines. Scale bars are 50 μm. (B) Immunohistochemical staining of MYC, CDK4 and TIAM1 in regenerating crypts from WT and *CIP2A*^{HOZ} intestines. Dashed line outlines crypt area used for histoscoring. Insert shows magnified image of MYC staining intensity in selected crypts. Scale bars are 50 μm. (C) Histoscoring of intensity of MYC immunopositivity in regenerating crypts crypts from WT and *CIP2A*^{HOZ} intestines. (p = not significant, Mann Whitney, n= 3 vs. 3). (D) qRT-PCR analysis for MYC in WT regenerating and *CIP2A*^{HOZ} regenerating small intestine (p = not significant, TTest, n=6). (E) Immunofluorescent staining for pS62MYC in WT, CIP2A^{HOZ}, WT regenerating and CIP2A^{HOZ} regenerating small intestine. Ki67 was co-stained to assess the induction of proliferation. Scale bars are 25 μm (F) Quantitation of pS62MYC intensity per cell from panel (E). (G) qRT-PCR analysis for MYC target gene expression in WT regenerating and *CIP2A*^{HOZ} regenerating small intestine (*p < 0.05, **p < 0.01, ***p < 0.001. TTest, n=3). Red line represents mRNA expression levels of MYC target genes normalized to 1, in wild type tissue. (H) Immunohistochemical staining of TIAM1 and CDK4 in regenerating crypts from WT, *CIP2A*^{HOZ} and *Myc*$^{fl/fl}$ intestines. Scale bars are 50 μm. (I) Histoscoring of CDK4 and TIAM1 immunopositivity in regenerating crypts from WT and *CIP2A*^{HOZ} intestines. (Mann Whitney, n= 6 vs 7). The data is derived from adjacent tissue section of those analysed for MYC histoscore in (B). Asterisk indicates an outlier value removed from the analyses.

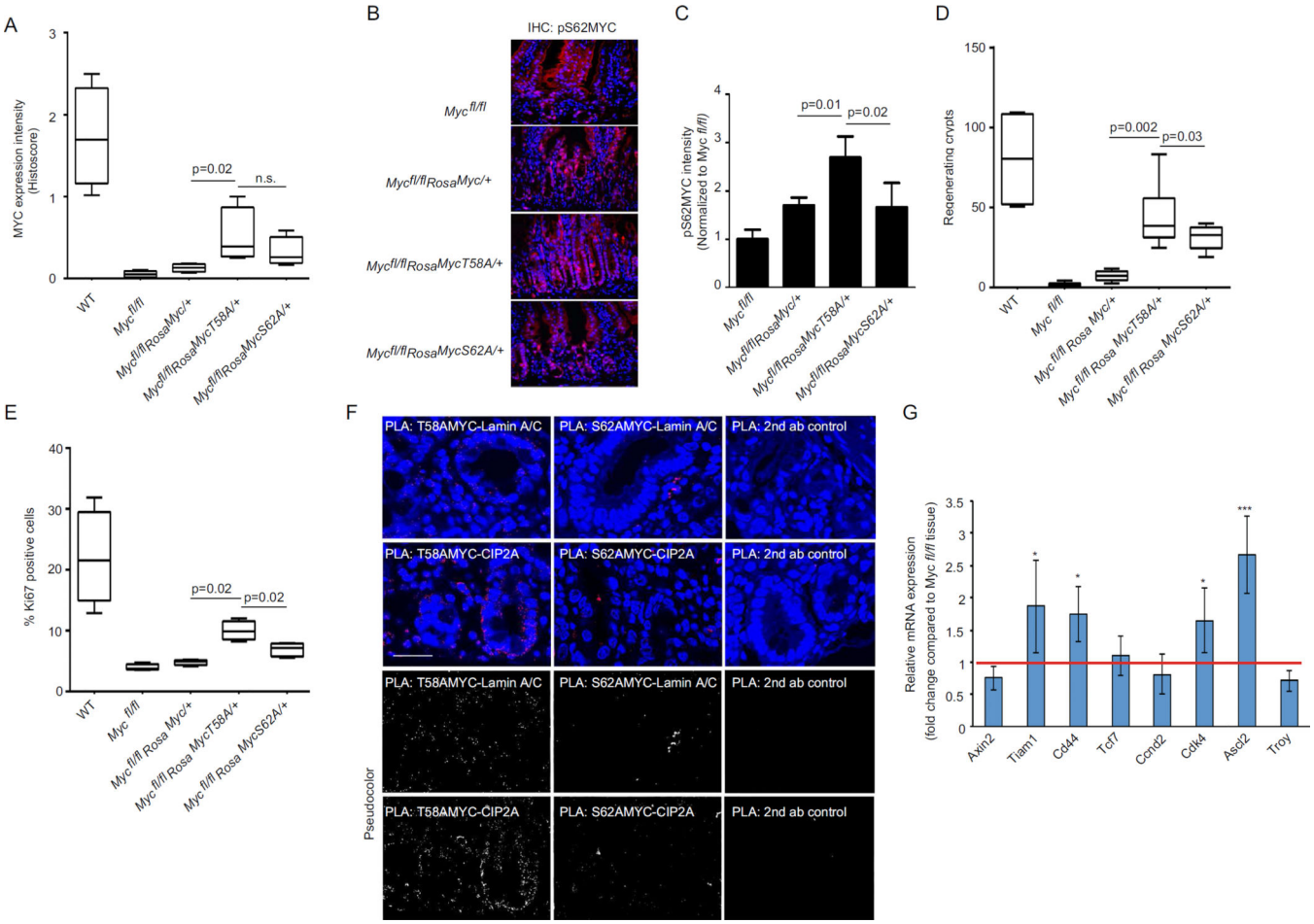

Figure 7. Analysis of MYC knock-in mutants support the importance of MYC serine 62 phosphorylation and Lamin A/C association for proliferation induction *in vivo*

(A) Quantitation of MYC immunostaining intensity in regenerating small intestine in mice with indicated genotypes. (n.s. = not significant, Mann Whitney, n= 4 vs. 4). (B) Immunofluorescent staining for pS62MYC in regenerating small intestine in mice with indicated genotypes. (C) Quantitation of pS62MYC intensity from panel (B) (Mann Whitney, n= 4 vs. 4). (D) Scoring of regenerating crypts in mice with indicated genotypes 72h post irradiation. (E) Scoring of percentage of Ki67 positive cells per crypt cells in mice with indicated genotypes 72h post irradiation. (F) PLA analysis of MYC-Lamin A/C and MYC-CIP2A association in intestinal crypts in mice with indicated genotypes 72h post irradiation. Specificity of PLA is shown by lack of PLA signals in secondary antibody only control panel. Scale bar is 25 μm. (G) qRT-PCR analysis for CIP2A-regulated MYC target gene expression in $Myc^{fl/fl}$ and $Myc^{fl/fl}$ $Rosa^{MycT58A/+}$ small intestine (*p < 0.05, **p < 0.01, ***p < 0.001. TTest, n=3). Red line represents mRNA expression levels of CIP2A-regulated MYC target genes normalized to 1 in $Myc^{fl/fl}$ small intestine.